Optical Engineering

OpticalEngineering.SPIEDigitalLibrary.org

Measurement of dynamic interferometer baseline perturbations by means of wavelength-scanning interferometry

Nikolai Ushakov
Leonid Liokumovich

SPIE.

Measurement of dynamic interferometer baseline perturbations by means of wavelength-scanning interferometry

Nikolai Ushakov* **and Leonid Liokumovich**
St. Petersburg State Polytechnical University, Polytechnicheskaya 29, St. Petersburg 195251, Russia

Abstract. An approach for measuring fast oscillations of an absolute value of interferometer optical path difference (OPD) has been developed. The principles of frequency-scanning interferometry are utilized for the registration of the interferometer spectral function from which the OPD is calculated. The proposed approach enables one to capture the absolute baseline variations at frequencies much higher than the spectral acquisition rate. Despite the conventional approaches associating a single baseline indication to the registered spectrum, in the proposed method, a specially developed demodulation procedure is applied to the spectrum. This provides the ability to capture the baseline variations that took place during the spectrum acquisition. An analytical model describing the limitations on the parameters of the possibly registered baseline variations is developed. The experimental verification of the proposed approach and the developed model has been performed. [DOI: 10.1117/1.OE.53.11.114103]

Keywords: fiber-optic sensors; interferometric signal demodulation; signal processing; extrinsic Fabry–Perot interferometer; spectral measurements; phase measurements; vibration measurement; wavelength-scanning interferometry.

Paper 141164P received Jul. 21, 2014; accepted for publication Oct. 23, 2014; published online Nov. 12, 2014.

1 Introduction

Fiber-optic interferometric sensors have been the subject of extensive study in academia and industry during the last three decades.[1] Their immunity to electromagnetic radiation, low cost, small dimensions, ability to operate in harsh environments, and high performance make them attractive for a great diversity of applications for measurement of temperature,[2] strain,[3] pressure,[4] humidity,[5] electric field,[6] and micro-displacements[7–9] in such areas as oil and gas exploitation,[4] structure health monitoring,[3] nuclear energetics,[10] and fundamental science.[8] The principle of the interferometric sensors is the relation of the measurable quantity x (strain, temperature, etc.) with the interferometer optical path difference (OPD) via either geometrical length $L(x)$ or refractive index $n(x)$ of the media in which the path difference is obtained.

In most of these applications, it is crucial to capture the absolute value of the interferometer OPD. This can be performed by either white-light[11] techniques utilizing a tunable read-out interferometer or approaches based on the registration and subsequent analysis of the interferometer spectral function. One of the most accurate spectral registering methods is wavelength-domain interferometry (WDI), demonstrating picometer-level resolutions, high absolute accuracies, and a large dynamic measurement range.[7,9] However, due to the limited time of spectrum measurement T_M and limited spectrum acquisition repetition frequency $F_S(F_S \geq 1/T_M)$, the sample rate may not be high enough for some applications, where higher speeds along with an absolute value and high resolution are essential. A feasible solution is to use a spectrometer with a higher acquisition rate. However, generally, such spectrometers are based on diffraction gratings and charge-coupled devices, which cannot provide a high spectral resolution and signal-to-noise ratio (SNR). Therefore, the resolution of such sensors will be significantly reduced. In the current paper, we develop an alternative technique based on a novel signal processing approach, enabling one to overcome the disadvantage of single point per spectrum measurement and track much faster baseline fluctuations than the spectrum acquisition rate.

In the WDI techniques, the optical spectral function of the interferometer is registered, which, for a two-beam interferometer (considering the low-finesse Fabry–Perot configuration with OPD $= 2nL$), is given by

$$S_I(L,\lambda) = S_0(L,\lambda) + S(L,\lambda), \tag{1}$$

$$S(L,\lambda) = S_M \cos[4\pi nL/\lambda + \gamma(L,\lambda)], \tag{2}$$

where $S_0 = I_1 + I_2$, $S_M = 2(I_1 I_2)^{1/2}$, I_1 and I_2 are the intensities of the interfering light beams; n is the refractive index of the media in which the propagation takes place; λ is the free-space light wavelength; the additional phase term $\gamma(L,\lambda)$ is induced by the phase shifts in the elements of the optical setup and a diffraction-induced phase shift if non-guided beam propagation takes place.

One of the most attractive approaches for estimation of the baseline L from the registered spectrum is to approximate its variable component $S'(\lambda)$ with analytical Eq. (2) by means of least-squares fitting. Such a fitting returns the global minimum of the residual norm, given by

$$R(L) = \|S'(\lambda) - S(L,\lambda)\| = \sqrt{\sum_i [S'_i - S_i(L)]^2}, \tag{3}$$

*Address all correspondence to: Nikolai Ushakov, E-mail: n.ushakoff@spbstu.ru

0091-3286/2014/$25.00 © 2014 SPIE

where $S'_i = S'(\lambda_i)$, $S_i(L) = S(\lambda_i, L)$, $\lambda_i = \lambda_0 + i\Delta$, Δ is the step between the spectral points, $i = -(M-1)/2,\ldots,(M-1)/2$, and M is the number of points in digitized spectrum (for the current notation M must be odd, which corresponds to the utilized interrogator and the performed simulations).

With the use of such an approximation-based approach, a resolution of an air-gap extrinsic fiber Fabry-Perot interferometer (EFPI) cavity length around 14 to 15 pm has been demonstrated.[12] However, the sample rate F_S of conventional spectral function-registering measurements are equal to the spectrum acquisition rate, which does not exceed several hertz.

2 Signal Processing

In the current paper, we propose a method of registering much more rapid fluctuations of the interferometer baseline. Let us consider that the WDI methods are used for interrogating the sensor, therefore, at each particular temporal moment $t_i \in [-T_M/2; T_M/2]$ (or i'th spectrum point) the wavelength λ_i can be written as $\lambda_i = \lambda_0 + k_\lambda \cdot t_i$, and the width of the wavelength scanning range $\Lambda = M\Delta$. It should be noted that the zero time moment $t = 0$ corresponds to $i = 0$ (the middle point of the spectrum) and the step between t_i moments is equal to $1/f_D$, where f_D is the sample rate of the acquired photodetector signal.

On this basis one can take into account the variation of the interferometer baseline during the spectrum acquisition time T_M. In this case, the variable part of the interferometer spectrum S'_I can be expressed as

$$S'[\lambda_i, L(t_i)] = S_M \cdot \cos\left\{\frac{4\pi n L(t_i)}{\lambda_i} + \gamma[L(t_i), \lambda_i]\right\} = S_M \cdot \cos\left\{\frac{4\pi n L_0}{\lambda_i} + \frac{4\pi n \cdot \delta L(t_i)}{\lambda_i} + \gamma[L(t_i), \lambda_i]\right\}, \tag{4}$$

where L_0 is the mean value of the interferometer baseline during spectrum acquisition, and $\delta L(t_i)$ is the baseline variation with respect to the mean L_0, further denoted as δL_i for simplicity.

For further convenience, we transition from the wavelength λ_i to the optical frequency $\nu_j = \nu_0 + k_\nu \cdot t_j$ in the interferometer spectrum expressions, as was done in, for instance, Ref. 13. It should be noted that the uniform grids of the wavelengths λ_i and the optical frequencies ν_j do not correspond to each other, since the uniform wavelength stepping with Δ produces a nonuniform frequency grid ($\nu_i = c/n\lambda_i$), and vice versa. In this paper, the index i will define the uniform wavelength grid, and the index j will define the uniform frequency grid. On this basis, the expression for the interferometer spectral function transforms to the following form:

$$S'_j(L_0) = S_M \cdot \cos\left[\frac{4\pi n L_0}{c}\nu_j + \frac{4\pi n \cdot \delta L_j}{c}\nu_j + \gamma_j\right]. \tag{5}$$

The structure of Eq. (5) is quite similar to the one for a quasi-harmonic signal with respect to the ν_j with carrier frequency f_C:

$$f_C = \frac{2nL_0k_\nu}{c} \approx \frac{2nL_0k_\lambda}{\lambda_0^2} \tag{6}$$

and angular modulation. It can be shown that the phase term γ_j exhibits a weak dependency on the OPD $\gamma_j(L)$, therefore, assuming $\delta L \ll L_0$, the effect of this additional phase modulation is quite weak and the influence of the baseline variations δL on the γ_j can be neglected. Throughout this paper, the following notation will be used: $\gamma_j = \gamma(L_0, c/\nu_j)$, $\gamma_i = \gamma(L_0, \lambda_i)$. For the case of the constant interferometer baseline, during the spectrum acquisition [Eq. (5)] transforms to

$$S_j(L_0) = S_M \cdot \cos\left(4\pi \cdot \frac{n}{c} L_0 \nu_j + \gamma_j\right). \tag{7}$$

This signal is quasi-harmonic since the argument increment is related not only to the equivalent frequency $2nL_0/c$, but also to the nonuniform term γ_j, whose behavior must be precisely calculated or can be verified experimentally.

Even in the presence of the δL perturbation, the signal S'_j remains quasi-harmonic and its argument can be obtained by means of the Hilbert transform. Comparing Eqs. (5) and (7), the signal processing for obtaining the δL_j from the measured spectrum S'_j can be divided into the following two steps:

1. Find the average baseline value L'_0 by means of approximating the measured spectrum S'_i by the analytical Eq. (2) (Eq. (7) can be applied to S'_j as well, if the spectrum is measured with respect to the optical frequency). A detailed description and analysis of the approximation method used in the current study are presented in Refs. 7 and 12. In the context of the argument demodulation task, this first step is essential for finding the carrier frequency f_C, necessary for the following demodulation of the baseline variations.
2. By means of the Hilbert transform calculate the analytic signal for the measured spectral function S'_j. After that obtain the argument of the analytic signal to which apply the standard unwrapping procedure based on the Itoh-criterion.[14] This will produce continuous argument ψ_j. Then the desired difference of the arguments is calculated as

$$\Psi_j = \psi_j - 4\pi n L_0 \nu_j / c - \gamma_j, \tag{8}$$

from which the baseline variation δL_j can be found according to the equation

$$\delta L_j = \frac{\Psi_j \cdot c}{4\pi n \nu_j}. \tag{9}$$

The use of the first step, obtaining the L_0 with very high accuracy, enables one to find the nonperturbation part of the ψ_j argument with much greater precision than detrending the ψ_j and other simple methods deleting the regular components of ψ_j.

It should be noted that, in practical optical spectrum analyzers the uniform wavelength grid is generally used, therefore, the corresponding optical frequency scale ν_i in Eqs. (5) and (7) will be related to temporal moments as $\nu_i = c/(\lambda_0 + k_\lambda t_i)$, resulting in incorrect calculations of

the analytical signals' phases and, therefore, an improper performance of the signal processing. In order to overcome this problem, two possible solutions can be proposed:

- Utilization of nonuniform fast Fourier transform algorithms[15] for analytical signal calculation.
- Interpolation of the initially registered spectrum $S'(\lambda_i)$ with the uniform wavelength scale to spectrum $S'(c/\nu_j)$ with the uniform frequency scale before analytic signal calculation. An inverse interpolation will be needed for the calculated δL_j signal in order to obtain the signal δL_i (and $L_i = L_0' + \delta L_i$), uniformly sampled with respect to time.

3 Method Limitations

For proper performance of the proposed approach, the limits on the spectrum and the amplitude of the baseline variation δL_j must be formulated. The applicability criterion is that the spectral components of the S_j' temporal representation do not decrease below zero and do satisfy the Nyquist limit. For simplicity, let us consider the limitations for the case of harmonic oscillation of the interferometer baseline with frequency f_L and amplitude L_m

$$\delta L_j = L_\mathrm{m}\cos(2\pi f_L t_j). \tag{10}$$

On the basis of Eq. (10), taking into account that the frequency scanning range $k_\nu \cdot T_\mathrm{M}$ is much smaller than the central optical frequency v_0 and omitting the quasi-stationary term γ_j, the total phase of S_j' can be expressed as

$$\begin{aligned}\psi(t_j) &= \frac{4\pi n L_0 k_\nu}{c} t_j + \frac{4\pi n \nu_0}{c} L_\mathrm{m}\cos(2\pi f_\mathrm{L} t_j)\\ &= 2\pi f_\mathrm{C} t_j + \psi_\mathrm{m}\cos(2\pi f_\mathrm{L} t_j).\end{aligned} \tag{11}$$

The spectrum width of the signal with argument [Eq. (11)] can be estimated according to Carson's bandwidth rule as a sum of the perturbation frequency f_L and frequency deviation $f_\mathrm{F} = 4\pi n \nu_0 f_\mathrm{L} L_\mathrm{m}/c$. For adequate representation of the digitized signal, the following restrictions on the baseline variations must be fulfilled $f_\mathrm{L} + f_\mathrm{F} < f_\mathrm{C}$, $f_\mathrm{L} + f_\mathrm{F} < f_\mathrm{D} - f_\mathrm{C}$. For typical values of f_D, L_0, and $k_\lambda(k_\nu)$, the second inequality is fulfilled by default, so only the first one is relevant, and is expressed as follows:

$$f_\mathrm{L}\cdot\left(1+\frac{4\pi n\nu_0}{c}L_\mathrm{m}\right) = f_\mathrm{L}\cdot\left(1+4\pi n\frac{L_\mathrm{m}}{\lambda_0}\right) < \frac{2nL_0k_\nu}{c} \approx \frac{2nL_0k_\lambda}{\lambda_0^2}. \tag{12}$$

For a certain device, this equation serves as a relation between the maximal values of f_L and L_m for a signal, which can be correctly measured by the proposed approach.

On the other hand, the level of the minimal possible detectable signal is determined by the noise level of the system. For that, the SNR of the measured spectral function S_j' must be determined as well as the relation of the noises of the initial spectrum S_j' and the noises of the resulting demodulated signal δL_j.

As is widely known, for an ideal phase detector, the resulting phase noise variance is related to the initial SNR of the phase modulated signal by[16]

$$\sigma_\varphi{}^2 = 0.5\cdot \mathrm{SNR}^{-1}, \tag{13}$$

for an SNR introduced as the ratio of signal and noise powers. The sense of this relation is quite similar to the one of a Cramer–Rao bound, giving the lower limit of a sampled noisy sinusoid estimated phase's variance.[17] It should be noted that the noise power is captured in the frequency band of the photodetector (or analog-to-digital converter, depending on which is broader). An analogy with a phase detector is applicable in our case, since the argument of the S_j' signal is found by means of a Hilbert transform during the calculation of the target signal δL_j. An analytical model describing the relation of the SNR of the registered spectral function with the parameters of the optical setup was developed in Ref. 12, where a particular case of EFPI with Gaussian beam assumption was considered. As in the current paper, the WDI was analyzed, therefore, the noise mechanisms can be considered the same, resulting in two main noise contributions:

- jitter of the wavelength points during the wavelength scan, caused by the fluctuations of the signal sampling moments, characterized by a random variables $\delta\lambda_i$ (or $\delta\lambda_j$ in the above used notation) with standard deviation $\sigma_{\delta\lambda}$;
- additive noises, produced by the photoregistering devices, light source intensity noises, etc., denoted as a normally distributed random term δs_i (or δs_j), $\sigma_s = \mathrm{stdev}\{\delta s\}$.

With this in mind, the resultant spectral function of the interferometer can be written in the following form:

$$\begin{aligned}S_\mathrm{I} &= S_0 + S_i' = I_1 + I_2\\ &\quad + 2\sqrt{I_1 I_2}\cos\left[\frac{4\pi n(L_0+\delta L_i)}{\lambda_i+\delta\lambda_i} + \gamma(L_0, \lambda_i+\delta\lambda_i)\right] + \delta s_i.\end{aligned} \tag{14}$$

Throughout this paper, the γ phase term will be approximated as $\gamma(L_0, \lambda_i)$, since, as shown in Sec. 2, its deviation due to δL_i is quite small, but on the other hand, its dependence on the wavelength is mainly a consequence of free beam propagation, while, as shown in Ref. 12 for an extrinsic Fabry–Perot interferometer, its influence on the resultant SNR of S_i' is negligible. Since the wavelength jitter and the laser intensity and photodetector noises are independent, we will consider these mechanisms separately and then will estimate their total influence on the sensor resolution.

As shown in Ref. 12 for the signal approach,[7] the spectral function distortion produced by the wavelength jitter can be interpreted as an additive noise, with SNR given by

$$\mathrm{SNR_J} = \frac{2\lambda_0^4}{(8\pi n L_0 \sigma_{\delta\lambda})^2}. \tag{15}$$

In order to consider the most general case, we will assume that the additive noise level depends on the mean optical power incident on the photodetector. A simple yet practical approximation of this dependence by a power function will be used

$$\sigma_s = aS_0^b. \tag{16}$$

The parameters a and b must be obtained explicitly for a given experimental setup. On this basis, the equation for SNR stipulated by the additive noises can be expressed as follows:

$$\mathrm{SNR_A} = \frac{S_\mathrm{M}^2/2}{\sigma_s^2} = \frac{2I_1I_2}{a^2\cdot(I_1+I_2)^{2b}} = \frac{V^2}{2a^2\cdot S_0^{2b-2}}, \tag{17}$$

where $V = 2(I_1I_2)^{1/2}/(I_1+I_2)$ is the visibility of the fringes in the interferometer spectrum, and $S_0 = I_1 + I_2$ is the optical power incident to the interferometer.

The resultant SNR will be given by

$$\mathrm{SNR_T} = (\mathrm{SNR_A^{-1}} + \mathrm{SNR_J^{-1}})^{-1}. \tag{18}$$

As a result, according to Eqs. (9), (13), and (18), the standard deviation of the baseline measurement noise σ can be expressed as

$$\begin{aligned}\sigma_\mathrm{F} &= \frac{\lambda_0}{4\pi n}\sigma_\varphi = \frac{\lambda_0}{4\sqrt{2}\pi n}(\mathrm{SNR_A^{-1}} + \mathrm{SNR_J^{-1}})^{1/2} \\ &= \frac{\lambda_0}{4\sqrt{2}\pi n}\sqrt{\frac{(8\pi n L_0\sigma_{\delta\lambda})^2}{\lambda_0^4} + \frac{4a^2S_0^{2b-2}}{V^2}}.\end{aligned} \tag{19}$$

The above equation can be used for estimating the lower bound of the detectable signal amplitude. In Eq. (19), it gives the standard deviation of the noises in the initial (broad) frequency band, determined by the sample rate of the photodetector and equal to $f_\mathrm{D}/2$. However, it is more convenient to consider the noises only in the frequency band of the target signal, introducing the noise spectral density. Assuming that the resulting noise samples after the Hilbert transform demodulation are uncorrelated, one can easily find the spectral density g_L of the OPD noises as

$$g_\mathrm{L} = \sigma_\mathrm{F}\cdot\sqrt{\frac{2}{f_\mathrm{D}}} = \frac{\lambda_0}{4\pi n}\sqrt{\frac{(8\pi n L_0\sigma_{\delta\lambda})^2}{\lambda_0^4} + \frac{4a^2S_0^{2b-2}}{V^2}}\cdot\sqrt{\frac{1}{2f_\mathrm{D}}}. \tag{20}$$

The OPD noise standard deviation σ_L can be found as a product of the spectral density g_L and square root of the target frequency bandwidth. For simplicity, the equivalent carrier frequency f_C [Eq. (6)] will be taken as the upper limit of the signal bandwidth. The resultant baseline noise in the target frequency band $[0, f_\mathrm{C}]$ is, therefore, given by

$$\sigma_\mathrm{L} = g_\mathrm{L}\cdot\sqrt{f_\mathrm{C}} = \frac{\lambda_0}{4\pi n}\sqrt{\frac{(8\pi n L_0\sigma_{\delta\lambda})^2}{\lambda_0^4} + \frac{4a^2P_0^{2b-2}}{V^2}}\cdot\sqrt{\frac{nL_0k_\lambda}{\lambda_0^2 f_\mathrm{D}}}. \tag{21}$$

Depending on a particular task, the resolution will be stipulated by different factors; however, it will still be related to the σ_L.

The estimates [Eqs. (20) and (21)] can be applied to a particular interferometric scheme if the visibility value V, generally dependent on the interferometer parameters, is specified. Below we will consider the case of a low-finesse EFPI, which can be approximated as a two-beam interferometer. In this case, the beam intensities are determined by the laser output power P_0, mirrors reflections and optical losses caused by the divergence of a nonguided beam and a coupling coefficient[12] $\eta(L_0)$ of this beam and the fiber mode: $I_1 = P_0\cdot R_1$, $I_2 = P_0\cdot R_2\cdot\eta(L_0)$. Under assumption of Gaussian profile of the fiber mode and the free beam, the coupling coefficient and the fringe visibility are given by

$$\begin{aligned}\eta &= \frac{(\pi n w_0^2)^2}{L^2\lambda^2 + (\pi n w_0^2)^2}, \\ V &= \frac{2\sqrt{R_1R_2}}{R_1\cdot[(L\lambda/\pi n w_0^2)^2 + 1]^{1/2} + R_2},\end{aligned} \tag{22}$$

where w_0 is the fiber mode field radius. In such a manner, the standard deviation of the OPD noise for EFPI is

$$\begin{aligned}\sigma_\mathrm{L} &= \frac{\lambda_0}{4\pi n}\sqrt{\frac{f_\mathrm{C}}{\mathrm{SNR_T}\cdot f_\mathrm{D}}} \\ &= \frac{\lambda_0}{4\pi n}\sqrt{\frac{(8\pi n L_0\sigma_{\delta\lambda})^2}{\lambda_0^4} + \frac{a^2[R_1 + R_2\eta(L_0)]^{2b}}{P_0^{2-2b}R_1R_2\eta(L_0)}}\cdot\sqrt{\frac{nL_0k_\lambda}{\lambda_0^2 f_\mathrm{D}}},\end{aligned} \tag{23}$$

where the equation for the coupling coefficient [Eq. (22)] was not substituted in order to avoid an excessive bulkiness.

The lower bound of the perturbation frequency is the simplest and is formulated as follows. For proper performance of the spectrum approximation approach[7] applied at the first step of the processing, the linear component of the baseline perturbation must be minimized, therefore, the period of the baseline oscillation must be less than or equal to the spectrum measurement time T_M. The rapid slope of the baseline during the spectrum measurement time results in an abrupt approximation error. An approach overcoming this issue was proposed and implemented in Ref. 18.

In order to achieve the resolutions given by Eqs. (21) and (23), the calculated baseline variation with uniform temporal sampling δL_i must be filtered by a low-pass filter with a cut-off frequency f_C. By doing so, the effort in displacement resolution will be $\sim(f_\mathrm{D}/2f_\mathrm{C})^{-1/2}$ for the case of white noise, which, for practical frequencies (see Sec. 4) is greater than one order. Recalling the approximating baseline estimation approach, it corresponds to the filtering performed with the lowest physically meaningful cut-off frequency $f_\mathrm{C} = 1/T_\mathrm{M}$. Let us note the correspondence between the obtained estimations [Eqs. (21) and (23)] and the quasi-static case, returning a single point for a measured spectral function (as done in Refs. 7, 9, 12, and 13): considering an extreme situation $f_\mathrm{C} = 1/T_\mathrm{M}$ and substituting it and $f_\mathrm{D} = M/T_\mathrm{M}$ into Eq. (23), one obtains

$$\sigma_\mathrm{L} = \frac{\lambda_0}{4\pi n}\sqrt{\frac{1}{\mathrm{SNR_T}\cdot M}} = \frac{\lambda_0}{4\pi n}\cdot\sigma_{\varphi\mathrm{CRLB}} = \sigma_{\mathrm{L\,CRLB}}, \tag{24}$$

where $\sigma_{\varphi\mathrm{CRLB}}$ is a Cramer–Rao bound[17] on the standard deviation of the estimate of a noisy sinusoid's phase; $\sigma_{\mathrm{L\,CRLB}}$—Cramer–Rao bound recalculated to the interferometer baseline domain. Substituting the parameters of the practical setup (see Sec. 4), one obtains the dependency

$\sigma_L \approx 0.9 \times 10^{-3} \cdot \mathrm{SNR}_T^{-1/2}$, which is in good accordance with the noise influence estimation on the resolution of the approximation-based baseline estimation approach obtained in Ref. 12, $\sigma_L = 1.1 \times 10^{-3} \cdot \mathrm{SNR}^{-1/2}$. Therefore, the conventional approximation-based techniques are a special case of the proposed one in the limit $f_C = 1/T_M$.

4 Experimental Demonstration

The proposed approach was implemented and tested experimentally. Spectra measurements were performed using the optical sensor interrogator National Instruments PXIe 4844, installed on PXI chassis PXIe 1065, controlled by PXIe 8106 controller. Spectrometer parameters are the following: scanning range $1510 \div 1590$ nm (spectral interval width $\Lambda = 80$ nm, mean wavelength $\lambda_0 = 1.55$ μm), spectral step $\Delta = 4$ pm (number of spectral points $M = 20001$), spectrum acquisition time $T_M \approx 0.035$ s, output power $P \approx 0.06$ mW, wavelength scanning speed $k_\lambda = 2.4$ μm/s, photodetector sample rate $f_D = 570$ kHz, and spectral points jitter $\sigma_{\delta\lambda} = 1$ pm. The parameters a and b for the current interrogator were found experimentally in Ref. 12 and have the following values: $a = 8.47 \times 10^{-4}$, $b = 0.81$. The experimental setup is schematically illustrated in Fig. 1. The examined interferometer was formed by the face of the SMF-28 fiber (reflectivity at the air-fused silica bound $R_1 = 3.5\%$) with mode field radius $w_0 = 5.2$ μm, packaged in an FC/PC connector and an external mirror with $R_2 \approx 90\%$, adjusted to the PZT actuator. The controlling voltage for the PZT was generated by the PXIe 5421 signal generator, which was installed on the same PXI chassis.

The efficiency of the utilized PZT actuator was approximately 100 nm/V in the frequency range 10 to 1000 Hz. The mean baseline value L_0 was varied within the interval 550 to 750 μm, resulting in the S_i' carrier frequency $f_{Sc} \approx 1100$ to 1500 Hz.

For the setup parameters mentioned above, relations of the amplitude L_m and frequency f_L limits for different baseline values L_0 are illustrated in Fig. 2. In the diagram in Fig. 2, the lower limit on the detectable amplitude was assumed $\sqrt{2} \cdot \sigma_L$, estimated according to Eq. (23) with the resulting SNR $= 1$. This condition can differ for different tasks and further signal processing. In such a manner, the final applicability limits will be determined by intersection of the criteria in Eqs. (12), (23), and $f_L > 1/T_M$.

In the performed experiments described below, a voltage with the following parameters was applied to the PZT:

- the excitation voltage amplitude was varied from 0.05 to 3 V, resulting in the EFPI baseline variation amplitudes from 5 nm to 0.3 μm;
- the frequency was varied from 50 to 1000 Hz;
- the oscillation shape was either harmonic or triangular.

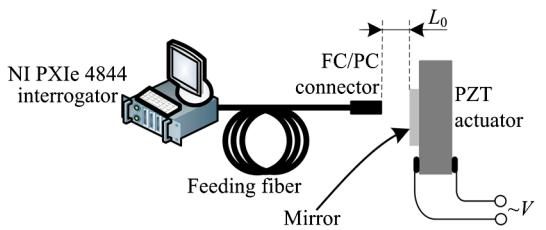

Fig. 1 Experimental setup.

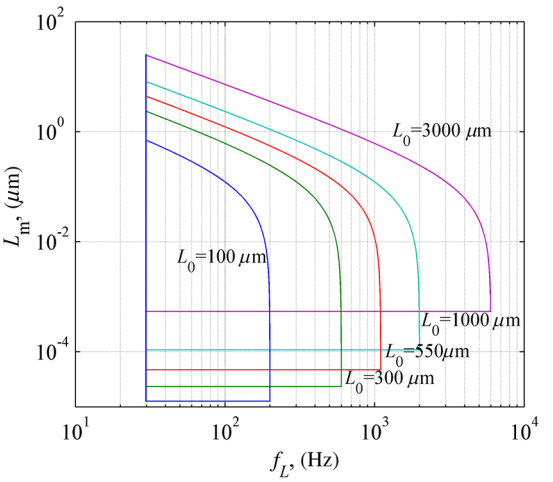

Fig. 2 Limits of the amplitude and frequency of the harmonic baseline variation for different baseline values.

The measured signals for the case of harmonic baseline oscillations with a mean baseline value $L_0 \approx 550$ μm are shown in Fig. 3. Three cases are demonstrated: frequency 200 Hz, amplitude 90 nm; frequency 200 Hz, amplitude 7 nm; frequency 800 Hz, and amplitude 12 nm.

In Fig. 4, the spectra of the above-shown signals are demonstrated. The attained noise spectral density, calculated as the median level of the signal spectra in the frequency band $[0, f_C]$ was $g_L' = 1.1$ pm/Hz$^{1/2}$, which is in a good correspondence with the value estimated according to Eq. (20) $g_L = 1.03$ pm/Hz$^{1/2}$. Considering the frequency band $[0, 1/T_M]$, corresponding to the approximation-based approach,[7,12] the level of captured noises will be $g_L/\sqrt{T_M} \sim 5.5$ pm, which is in accordance with the observed noise-influenced value reported in Ref. 12.

The experimental signals for the other parameters of the perturbation (triangular variations of the baseline) and the setup (other mean baseline values) can be found in Ref. 19 and the corresponding results are also in good correspondence with the predictions of the developed theoretical model.

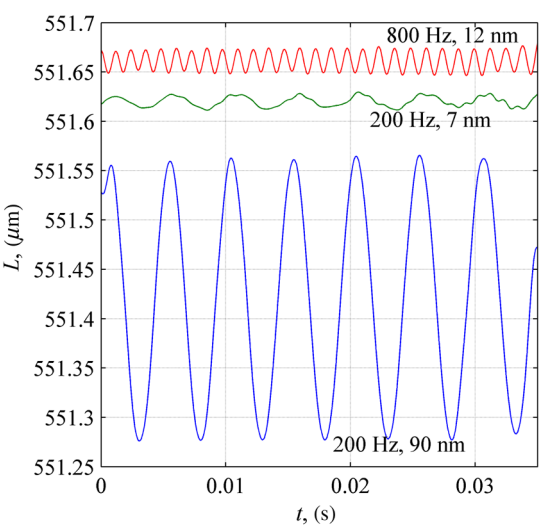

Fig. 3 Measured baseline variations.

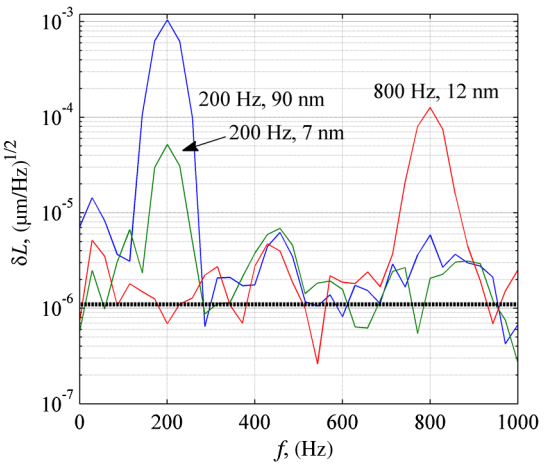

Fig. 4 Spectral density of the measured baseline oscillations for $L_0 \approx 550$ μm (solid lines), noise spectral density estimated according to Eq. (20) (dotted line).

5 Conclusions

In the current paper, an approach is proposed enabling one to overcome the conventional limitations of the wavelength-domain absolute interferometry where a single baseline value is obtained according to a single acquired interferometer spectrum. Instead, using the proposed signal processing approach, one is able to track the fast deviations of the absolute baseline value that take place during the spectrum acquisition. The upper limits on the frequency and amplitude of the perturbation are stipulated by the no-aliasing conditions and are related to the mean baseline value L_0. The lower limit on the signal frequency is determined by the spectrum measurement time T_M and inquires that the perturbation frequency $f_L > 1/T_M$. The lower limit on the signal amplitude is determined by the SNR of the measured interferometer spectrum and an analytical model relating the baseline resolution with the optical setup parameters was established. An experimental demonstration of the proposed baseline measurement approach with the extrinsic Fabry–Perot interferometer was performed and the attained resolution is in good agreement with the estimations performed with the developed model.

References

1. E. Udd, *Fiber Optic Sensors: An Introduction for Engineers and Scientists*, 2nd ed., pp. 119–372, John Wiley & Sons, Inc., Hoboken, New Jersey (2011).
2. G. Zhang, M. Yang, and M. Wang, "Large temperature sensitivity of fiber-optic extrinsic Fabry–Perot interferometer based on polymer-filled glass capillary," *Opt. Fiber Technol.* **19**, 618–622 (2013).
3. Y. Huang et al., "An extrinsic Fabry–Perot interferometer-based large strain sensor with high resolution," *Meas. Sci. Technol.* **21**(10), 105308 (2010).
4. R. D. Pechstedt, "Fibre optic pressure and temperature sensor for applications in harsh environments," *Proc. SPIE* **8794**, 879405 (2013).
5. R. Willsch et al., "Nanostructure-based optical fibre sensor systems and examples of their application," *Proc. SPIE* **6585**, 65850B (2007).
6. L. B. Liokumovich, A. V. Medvedev, and V. M. Petrov, "Fiber-optic polarization interferometer with an additional phase modulation for electric field measurements," *Opt. Mem. Neural Networks* **22**(1), 21–27 (2013).
7. N. Ushakov, L. Liokumovich, and A. Medvedev, "EFPI signal processing method providing picometer-level resolution in cavity length measurement," *Proc. SPIE* **8789**, 87890Y (2013).
8. V. Petrov et al., "Optical detection of the Casimir force between macroscopic objects," *Opt. Lett.* **31**(21), 3167–3169 (2006).
9. X. Zhou and Q. Yu, "Wide-range displacement sensor based on fiber-optic Fabry–Perot interferometer for subnanometer measurement," *IEEE Sens. J.* **11**(7), 1602–1606 (2011).
10. G. Cheymol et al., "Fibre optic extensometer for high radiation and high temperature nuclear applications," *IEEE Trans. Nucl. Sci.* **60**(5), 3781–3784 (2013).
11. Y. Yuan et al., "Tunable optical-path correlator for distributed strain or temperature-sensing application," *Opt. Lett.* **35**(20), 3357–3359 (2010).
12. N. Ushakov and L. Liokumovich, "Resolution limits of extrinsic Fabry–Perot interferometric displacement sensors utilizing wavelength scanning interrogation," *Appl. Opt.* **53**(23), 5092 (2014).
13. Zh. Wang et al., "Fourier transform white-light interferometry based on nonlinear wavelength sampling," *Opt. Eng.* **52**(10), 104102 (2013).
14. K. Itoh, "Analysis of the phase unwrapping algorithm," *Appl. Opt.* **21**(14), 2470 (1982).
15. M. Jacob, "Optimized least-square nonuniform fast Fourier transform," *IEEE Trans. Signal Process.* **57**(6), 2165–2177 (2009).
16. W. R. Davenport and W. L. Root, *An Introduction to the Theory of Random Signals and Noise*, John Wiley & Sons, Inc., New York (1987).
17. H. Fu and P. Y. Kam, "MAP/ML estimation of the frequency and phase of a single sinusoid in noise," *IEEE Trans. Signal Process.* **55**(3), 834–845 (2007).
18. E. A. Moro, M. D. Todd, and A. D. Puckett, "Understanding the effects of Doppler phenomena in white light Fabry–Perot interferometers for simultaneous position and velocity measurement," *Appl. Opt.* **51**(27), 6518–6527 (2012).
19. N. Ushakov and L. Liokumovich, "EFPI sensor utilizing optical spectrum analyzer with tunable laser: detection of baseline oscillations faster than spectrum acquisition rate," *Proc. SPIE* **9141**, 914116 (2014).

Nikolai Ushakov received a MS degree in 2011 from St. Petersburg Polytechnical University. His thesis was dedicated to Raman Spectroscopy. He is currently working toward a PhD degree on interferometric fiber-optic sensors in St. Petersburg Polytechnical University, Radiophysics Department. His scientific interests include interferometric measurement techniques and digital signal processing.

Leonid Liokumovich defended his candidate of science and doctor of science dissertations in 1995 and 2008, respectively, at St. Petersburg Polytechnical University. Currently, he is a professor at the Radiophysics Department, St. Petersburg Polytechnical University. His scientific interests include interferometric and distributed optical fiber sensors, polarization measurements, and optical signals detection techniques.